Frequency-dependent reflections from a layer with attenuation caused by interlayer flow

Beatriz Quintal and Stefan M. Schmalholz, ETH Zurich*

Summary

We study the combined effect of (1) attenuation caused by interlayer-flow and (2) tuning on the reflection coefficient of a layer embedded in an elastic medium in one dimension. Both attenuation and tuning are frequency dependent. We only consider a contrast in attenuation between the layer and the non-attenuating medium. We use the analytical interlayer-flow model, which is based on Biot's theory of poroelasticity, to model attenuation in the layer. The resulting complex velocity for the attenuating layer is used in the analytical solution for the complex reflection coefficient of a layer embedded in an elastic medium. Attenuation combined with tuning in layers can generate reflection coefficients with significant (1) amplitude (> 10 %) and (2) frequency dependence. Our results can be applied to hydrocarbon reservoirs with high attenuation but low acoustic impedance contrast to the surrounding rock.

Introduction

We present a study on the frequency-dependent reflection coefficient of a layer exhibiting attenuation caused by interlayer flow (White et al., 1975). Quintal et al. (2009) showed that, for a wide range of realistic petrophysical parameters for sandstones partially saturated with water and gas, the quality factor, Q (wave attenuation can be defined as Q^{-1}), can be as small as 2 in the interlayer-flow model. They applied the interlayer-flow model to study the reflection coefficient, R, of a thin (compared to the wavelength) layer partially saturated with water and gas, exhibiting such high attenuation. The amplitude of the reflection coefficient of such a layer, due to contrast in attenuation to the non-attenuating background medium, but no acoustic (real part of) impedance contrast, can be greater than 10 % for a value of Q lower than 4.

In this paper, we extend the study made by Quintal et al. (2009), taking also into account the influence of the layer thickness on the amplitude of the reflection coefficient. The reflection coefficient of an elastic layer is frequency-dependent due to constructive and destructive interferences of waves reflected from the top and bottom of the layer (e.g., Kallweit and Wood, 1982). This effect is referred to as tuning. The reflection coefficient of a layer with frequency-dependent attenuation is then influenced by two frequency-dependent mechanisms: tuning and attenuation.

The reflection coefficient of an attenuating layer has a maximum when the transition and the tuning frequencies are identical. The transition frequency is the frequency at which attenuation is maximal; and the tuning frequency occurs when the positive and negative interferences result in the maximum amplitude of the reflected wave.

Here we study the combined effect of attenuation and tuning on the reflection coefficient of a layer exhibiting high attenuation contrast to the background medium, but no acoustic impedance contrast. To investigate the combined effect of frequency-dependent attenuation and tuning on the reflectivity of a layer, we use: (1) the analytical solution of the interlayer-flow model (White et al., 1975; Carcione and Picotti, 2006), simulating the influence of the frequency-dependent attenuation; and (2) a 1D analytical solution of the reflection coefficient of a layer embedded in an elastic medium (Brekhovskikh, 1980), where we vary the layer thickness with respect to the wavelength, simulating the influence of tuning.

The frequency-dependent *Q* of the interlayer-flow model

The interlayer-flow model, or 1D White model (White et al., 1975; Norris, 1993; Pride 2004; Müller and Gurevich, 2005; Carcione and Picotti, 2006; Carcione, 2007), is a physically based model for seismic wave attenuation in the low-frequency range. It can be solved with the Biot's equations of poroelasticity (Biot, 1962) with spatially varying petrophysical parameters (Dutta and Odé, 1979a, b; Dutta and Seriff, 1979). In the interlayer-flow model, attenuation and velocity dispersion can be explained by the combined effect of mesoscopic-scale (scale much larger than the pore size but much smaller than the wavelength) inhomogeneities and energy transfer between wave modes, i.e, conversion of fast P-wave to slow P-wave.

A partially saturated rock is represented, in the interlayer-flow model, by two periodically alternating layers of media 1 and 2. Each layer is a fully saturated poroelastic solid that differs by the pore fluid properties. Attenuation and dispersion of the phase velocity are caused by wave-induced fluid flow, generated by pressure differences between the layers. The analytical solution for the interlayer-flow model yields the frequency-dependent quality factor, Q, and phase velocity, V_P, (Carcione and Picotti, 2006):

$$Q = \mathrm{Re}(E)/\mathrm{Im}(E)\,, \tag{1}$$

$$V_P = (\mathrm{Re}(1/V))^{-1}\,, \tag{2}$$

where E is the complex modulus for a P-wave traveling along the direction perpendicular to the layering, and V is the complex velocity, or

$$V = \sqrt{E/\rho}\,, \quad (3)$$

where ρ is the bulk density of the partially saturated rock. Quintal et al. (2009) rearranged the equations of the analytical solution of the interlayer-flow model, defining E as the product of a real number, E_0, and a complex number, b,

$$E = E_0 b\,, \quad (4)$$

$$E_0 = \left(p_1/E_{G1} + p_2/E_{G2} \right)^{-1}, \quad (5)$$

$$b = \left(1 + (I_1 g_1 + I_2 g_2)^{-1}\right)^{-1}, \quad (6)$$

so that Q can be expressed as

$$Q = \mathrm{Re}(b)/\mathrm{Im}(b)\,. \quad (7)$$

The indexes 1 and 2 refer to the two different porous media, i.e., the two periodically alternating layers. For each saturated porous medium (j = 1, 2):

$$g_j = K_{Ej} \Big/ \left(2E_0 (r_2 - r_1)^2 p_j \right), \quad (8)$$

$$I_j = \sqrt{i\omega s_j}\, \coth\left(i\omega s_j / 2 \right), \quad (9)$$

$$s_j = \eta_j d_j^2 \big/ (K_{Ej} k_j)\,, \quad (10)$$

where $p_j = d_j/(d_1+d_2)$, and d_j is the layer thickness. Table 1 shows the symbols used for the basic petrophysical parameters, and the remaining parameters are defined in Table 2, with the index j omitted for clarity.

The quality factor in equation 7 is expressed as a function of two groups of petrophysical parameters, s and g, and the angular frequency, ω. The parameter s (equation 10) is dominated by the flow parameters, viscosity and permeability, and g (equation 8) consists mostly of elastic moduli and porosity. In the interlayer-flow model, Q has always a minimum, $Q_{\min}$, at a frequency referred to as transition frequency, f_{tr}. An approximation for f_{tr} was given by Dutta and Seriff (1979), for a rock partially saturated with water and gas:

$$f_{tr} \approx \frac{8 k_1 K_{E1}}{\pi \eta_1 d_1^2} = \frac{8}{\pi s_1}\,, \quad (11)$$

where index 1 refers to the water-saturated layer. Also for a rock partially saturated with water and gas, Quintal et al. (2009) showed that the value of $Q_{\min}$ can be approximated as a linear function of only the parameter g, and that the optimal patch-size ratio (or saturation ratio) that yields the lowest value of $Q_{\min}$ for a certain set of petrophysical parameters is:

$$\left(\frac{d_2}{d_1} \right)^{\min} = \sqrt{\frac{E_{G2} K_{E2}}{E_{G1} K_{E1}}}\,, \quad (12)$$

where indexes 1 and 2 refer to water and gas saturation, respectively.

Table 1. Symbols used for the petrophysical parameters.

Symbol	Parameter
ϕ	Porosity
K_m	Bulk modulus of dry frame
μ_m	Shear modulus of dry frame
K_s	Bulk modulus of the grain
μ_s	Shear modulus of the grain
K_f	Bulk modulus of the pore fluid
η	Viscosity of the pore fluid
k	Permeability of the porous rock
ρ_s	Density of the grain

Table 2. Definition of some parameters.

Definition	Parameter
$E_G = K_G + 4\mu_m/3$	P-wave modulus of the saturated rock
$K_E = E_m M / E_G$	Effective modulus
$r = \alpha M / E_G$	Ratio P-wave fluid tension to total normal stress
$K_G = K_m + \alpha^2 M$	Gassmann modulus
$E_m = K_m + 4\mu_m/3$	Dry-rock P-wave modulus
$M = \left(\frac{\alpha - \phi}{K_s} + \frac{\phi}{K_f} \right)^{-1}$	Solid-grain bulk modulus
$\alpha = 1 - K_m/K_s$	Biot's elastic parameter

The frequency-dependent *R* of a layer

The frequency-dependent reflection coefficient, R, can be calculated with a 1D analytical solution for a layer embedded in an elastic medium (e.g., Brekhovskikh, 1980):

$$R = \frac{1-z}{1+z}\left(1 - \frac{4z\,\mathrm{e}^{-i2h\omega/V_l}}{(1+z)^2 - (1-z)^2\,\mathrm{e}^{-i2h\omega/V_l}} \right), \quad (13)$$

where h is the layer thickness, and $z = V_l\rho_l/V_b\rho_b$ is the impedance ratio. The subscript l refers to the layer, and b corresponds to the background medium. When the layer exhibits attenuation, the velocity in the layer, V_l, is complex. The magnitude of the reflection coefficient is the absolute value of R, or $|R|$.

The combined effect of tuning and attenuation

In our study, a partially saturated layer exhibiting attenuation caused by interlayer flow is embedded in a non-attenuating background medium. We consider a model setup with no acoustic (real part of) impedance contrast between the layer and the background medium, only attenuation contrast.

We use equation 13 and the analytical solution of the interlayer-flow model (equations 1 to 10) to study the combined effect of the frequency-dependent attenuation and tuning on the reflectivity of a layer. When the layer exhibits attenuation (a finite value of Q, equation 1), the wave velocity (equation 3) is complex. For the wave velocity in the layer, V_l in equation 13, we use the complex velocity from equation 3, and for the velocity in the background medium, V_b in equation 13, we use the real part of the velocity in the layer, i.e., the phase velocity (equation 2). The density of the background medium and the bulk density of the saturated layer are the same.

The petrophysical properties of the layer are shown in Table 3 and correspond to sandstone partially saturated with water and gas. We use Pride's relations (Pride, 2003) to calculate K_m and μ_m. In Pride's relations, K_m and μ_m are related to K_s and μ_s through porosity and a parameter c, which is related to the degree of consolidation between grains. We choose c = 48, implying in a very poorly consolidated sandstone.

Table 3. Petrophysical parameters used in this study.

Rock matrix	Sandstone	
K_s (GPa)	36	
k (mD)	300	
ρ_s (kg/m^3)	2650	
ϕ	0.35	
Fluid constituent	Water	Gas
K_f (GPa)	2.4	0.022
ρ_f (kg/m^3)	1000	100
η (Pa s)	0.001	10^{-5}

We calculate the saturation ratio (or patch-size ratio) (equation 12) that yields the lowest value of $Q_{\min}$ for our set of parameters, which corresponds to 9 % of gas saturation in the layer; and we choose a heterogeneity size (d_1+d_2) of 0.48 m. Then, the partially saturated layer is composed of periodically alternating layers fully saturated with gas and water, the gas-saturated layers being 0.04-m thick (d_2), and the water-saturated ones, 0.44-m thick (d_1).

For the chosen petrophysical parameters and heterogeneity size, the value of $Q_{\min}$ is 3.5 and occurs at 8.5 Hz. Such a high attenuation is caused by wave-induced fluid flow between the layers saturated with water and gas, due to their significantly varying compressibilities (Table 3). Calculating the related complex velocity, and by varying the layer thickness with respect to the wavelength in equation 13, we calculate the reflection coefficient of the layer as a function of h/λ and f/f_{tr}, where λ is the wavelength and f is the frequency (Figure 1).

In Figure 1 we see that, for our set of parameters that yields $Q_{\min}$ = 3.5 at f_{tr} = 8.5 Hz, the maximum value of the reflection coefficient is about 11.5 %, and occurs when the transition frequency, f_{tr}, is equal to the tuning frequency, which corresponds to $\lambda = 4.3h$.

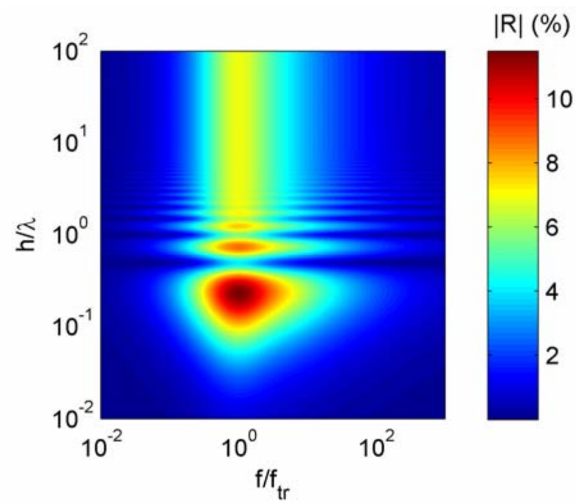

Figure 1. Absolute value of the reflection coefficient, R, of a layer due to the combined effect of tuning and frequency-dependent attenuation in the layer, when there is a high attenuation contrast between the layer and the background medium, but no acoustic impedance contrast. The petrophysical parameters for the layer correspond to poorly consolidated sandstone, partially saturated with 91 % water and 9 % gas. For the chosen parameters set, $Q_{\min}$ = 3.5 and f_{tr} = 8.5 Hz. The maximum $|R|$ is about 11.5 %, at $f = f_{tr}$ and when $\lambda = 4.3h$.

Discussion

High values of attenuation in hydrocarbon reservoirs have often been observed at seismic frequencies (e.g., Klimentos, 1995; Dasgupta and Clark, 1998; Rapoport et al., 2004), and related reflections in the low-frequency range have recently attracted an increased interest in the scientific and industrial communities (e.g., Goloshubin et al., 2006). Therefore, our study of reflections from a layer exhibiting high attenuation, caused by interlayer flow, can be applied to hydrocarbon reservoirs.

For partial water/gas saturation, the highest attenuation occurs for a small amount of gas, about 9 % (Quintal et al., 2009). Zones of small gas saturation and high attenuation, for example, may be located around the hydrocarbon reservoir at the water/gas or oil/gas contacts where the saturation changes gradually. Goloshubin et al. (2006) used some examples of field-data processing to show that hydrocarbon reservoirs exhibit increased reflective properties at low frequencies, and that expanding the active seismic bandwidth to low frequencies has a strong potential for predicting fluid content. Our analytical study shows that when the acoustic impedance contrast between a layer with high attenuation and the surrounding medium is negligible, the layer might be "invisible" in a certain frequency range, but it might exhibit significant reflectivity at another frequency at which its attenuation is high. A variation of one order of magnitude in the transition frequency can easily occur, since it is directly proportional to the permeability (equation 11), and variations of that order are commonly observed in the permeability of hydrocarbon reservoirs (normally from 100 mD to 1 D). We see in Figure 1 that a variation of one order of magnitude in frequency, around the transition frequency, corresponds to a variation of one order of magnitude in the absolute value of the reflection coefficient. For example, an attenuating layer, not visible in a seismic section where frequencies lower than 15 Hz are filtered out, could be visible at around 8 to 12 Hz. A seismic section can exhibit significantly different reflectors' pattern at different frequency ranges.

Conclusions

The combined effects of frequency-dependent attenuation, caused by interlayer flow, and tuning can yield reflection coefficients with significant amplitude (in our example, 11.5 %) and strong frequency dependence, for a layer exhibiting high attenuation contrast to the surrounding medium, but no acoustic impedance contrast. We showed that a variation in frequency of one order of magnitude can correspond to a variation of also one order of magnitude in the amplitude of the reflection coefficient.

Acknowledgements

This research was supported by ETH Zurich, KTI/CTI (The Innovation Promotion Agency in Switzerland), and Spectraseis. We thank Brad Artman for reviewing this manuscript.

References

Biot, M. A., 1962, Mechanics of deformation and acoustic propagation in porous media: Journal of Applied Physics, **33**, 1482-1498.

Brekhovskikh, L. M., 1980, Waves in Layered Media: Academic Press.

Carcione, J. M., and S. Picotti, 2006, P-wave seismic attenuation by slow-wave diffusion: Effects of inhomogeneous rock properties: Geophysics, **71**, O1-O8.

Carcione, J. M., 2007, Wave Fields in Real Media: Wave propagation in anisotropic, anelastic, porous and electromagnetic media, Handbook of Geophysical Exploration, **38**, Elsevier.

Dasgupta, R., and R. A. Clark, 1998, Estimation of *Q* from surface seismic reflection data: Geophysics, **63**, 2120-2128.

Dutta, N. C., and H. Odé, 1979a, Attenuation and dispersion of compressional waves in fluid filled porous rocks with partial gas saturation (White model) – Part I: Results: Geophysics, **44**, 1777-1788.

Dutta, N. C., and H. Odé, 1979b, Attenuation and dispersion of compressional waves in fluid filled porous rocks with partial gas saturation (White model) – Part II: Results: Geophysics, **44**, 1789-1805.

Dutta, N. C., and A. J. Seriff, 1979, On White's model of attenuation in rocks with partial gas saturation: Geophysics, **44**, 1806-1812.

Goloshubin, G., C. Van Schuyver, V. Korneev, D. Silin, and V. Vingalov, 2006, Reservoir imaging using low frequencies of seismic reflections: The Leading Edge, **25**, 527-531.

Kallweit, R. S., and L. C. Wood, 1982, The limits of resolution of zero-phase wavelets: Geophysics, **47**, 1035-1046.

Klimentos, T., 1995, Attenuation of P- and S-waves as a method of distinguishing gas and condensate from oil and water: Geophysics, **60**, 447-458.

Müller, T. M., and B. Gurevich, 2005, Wave-induced fluid flow in random porous media: Attenuation and dispersion of elastic waves: Journal of the Acoustical Society of America, **117**, 2732-2741.

Norris, A. N., 1993, Low-frequency dispersion and attenuation in partially saturated rocks: Journal of Acoustical Society of America, **94**, 359-370.

Pride, S. R., 2003, Relationships between seismic and hydrological properties, *in* Y. Rubin and S. Hubbard, eds., Hydrogeophysics: Springer, 253-290.

Pride, S. R., J. G. Berryman, and J. M. Harris, 2004, Seismic attenuation due to wave-induced flow: Journal of Geophysical Research, **109**, B01201, doi:10.1029/2003JB002639.

Quintal, B., S. M. Schmalholz, and Y. Y. Podladchikov, 2009, Low-frequency reflections from a thin layer with high attenuation caused by interlayer flow: Geophysics, **74**, N15-N23.

Rapoport, M. B., L. I. Rapoport, and V. I. Ryjkov, 2004, Direct detection of oil and gas fields based on seismic inelasticity effect: The Leading Edge, **23**, 276-278.

White, J. E., N. G. Mikhaylova, and F. M. Lyakhovitskiy, 1975, Low-frequency seismic waves in fluid saturated layered rocks: Izvestija Academy of Sciences USSR, Physics of the Solid Earth, **11**, 654-659.